ACS Combinatorial Science

RESEARCH ARTICLE

pubs.acs.org/acscombsci

Fluorescence Response Profiling for Small Molecule Sensors Utilizing the Green Fluorescent Protein Chromophore and Its Derivatives

Jun-Seok Lee,[†,#,▽] Anthony Baldridge,[⊥,▽] Suihan Feng,[†,‡] Yang SiQiang,[∥] Yun Kyung Kim,[†,#] Laren M. Tolbert,[*,⊥] and Young-Tae Chang[*,†,‡,∥]

[†]Department of Chemistry, [‡]MedChem Program of Life Sciences Institute, National University of Singapore, 3 Science Drive 3, Singapore 117543, Singapore

[∥]Laboratory of Bioimaging Probe Development, Singapore Bioimaging Consortium, Agency for Science, Technology and Research (A*STAR), Biopolis 138667, Singapore

[⊥]School of Chemistry and Biochemistry, Georgia Institute of Technology, Atlanta, Georgia 30332-0400, United States

[#]Life/Health Division, Integrated Omics Center, Korea Institute of Science and Technology (KIST), Seoul 136-791, South Korea

Supporting Information

ABSTRACT: Using a fluorescence response profile, a systematic examination was performed for synthetic chromophores of the green fluorescent protein (GFP) to discover new small molecule sensors. A group of 41 benzylideneimidazolinone compounds (**BDI**) was prepared and screened toward 94 biologically relevant analytes to generate fluorescence response profiles. From the response pattern, compounds containing aminobenzyl and heteroaromatic cyclic substructures revealed a pH dependent emission decrease effect, and unlike other fluorescence scaffolds, most **BDIs** showed fluorescence quenching when mixed with proteins. On the basis of the primary response profile, we obtained three selective fluorescence turn-on sensors for pH, human serum albumin (HSA), and total ribonucleic acid (RNA). Following analysis, a fluorescence response profile testing four nucleic acids revealed the alkyloxy (Ph−OR) functional group in the *para* position of benzyl analogues contributes to RNA selectivity. Among the primary hit compounds, **BDI 2** showed outstanding selectivity toward total RNA with 5-fold emission enhancement. Finally, **BDI 24** showed selective fluorescence increase to HSA (K_d = 3.57 μM) with a blue-shifted emission max wavelength ($\Delta\lambda_{em}$ = 15 nm). These examples of fluorescence sensor discovery by large-scale fluorescence response profiling demonstrate the general applicability of this approach and the usefulness of the response profiles.

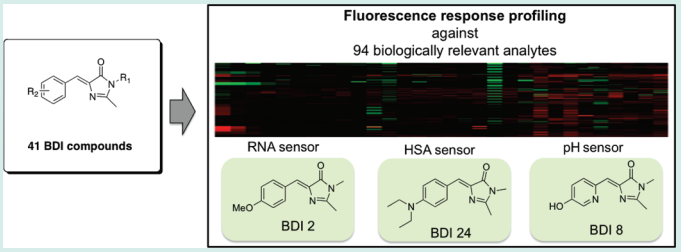

KEYWORDS: small molecule sensors, green fluorescent protein chromophore, fluorescence response profiling

INTRODUCTION

The green fluorescent protein (GFP) has attracted great attention as a fluorescent probe to study diverse problems in molecular biology.[1] Taking advantage of the autocatalytic cyclization and oxidation of three amino acid residues to form a natural chromophore (*p*-hydroxybenzylideneimidazolone, *p*-HBDI),[2] GFP generates a very effective and intense fluorescence signal. Nevertheless, investigation of the chromophore reveals distinct differences in fluorescent properties between wild type GFP (wt GFP) and the synthetic chromophore. The fluorescent quantum yield of the synthetic chromophore is much less and shows solvent and temperature dependence.[3] Studies suggest that the GFP β-barrel structure plays a critical role in protecting the chromophore and reducing conformational flexibility and thus diminishing the rate of radiationless decay. Within the rigid β-barrel structure, *p*-HBDI undergoes excited-state proton transfer (ESPT)[4] from the chromophore to the adjacent residue, E222,[5] resulting in very efficient emission from the anionic form. To exploit the GFP chromophore as a sensor, this environment-sensitive fluorescence turn-on phenomenon is utilized in several bimolecular fluorescence protein sensors.[6] However, the chromophore itself is rarely scrutinized to detect analyte molecules directly.

We envisioned that synthetic GFP chromophore derivatives have superior potential as small molecule fluorescent sensors, because of their desirable characteristics such as extremely low background in aqueous solution and high environmental sensitivity. Low background sensors are favorable in many applications because of their high signal-to-noise ratio.[7] Recently, the Burgess group has demonstrated that, by incorporating an *ortho*-aryl BF_2 group which complexes with the imidazolone nitrogen, the conformation of the chromophore can be frozen and the emission turned on.[8] Similarly, Chou has demonstrated that incorporation of an *ortho* hydroxyl group can turn on the emission through intramolecular hydrogen bonding, leading in the latter case to excited-state proton transfer.[9] We concluded

Received: September 22, 2010
Published: November 9, 2010

that such fluorescent turn-on detection for target molecules could be attained by specific interactions between GFP chromophores and analyte molecules, which instead of freezing the conformation intrinsically through the structure of the chromophore, instead freezes the conformation after complexation with the analyte. Indeed, recently we observed that proper construction of a hydrophobic chromophore could increase the fluorescence response by a factor of 15.[10] Accordingly, it would be of interest to investigate the chromophore modes of interaction with endogenous biomolecules, despite most previous studies, which focused on the nature of chromophore within the β-barrel in wt GFP. In this paper, we report a systematic analysis of the fluorescence change of the GFP chromophore and its derivatives when applied for sensing of biologically relevant analytes.

To develop an effective fluorescent sensor, an important criterion that must be met is high selectivity for a target molecule. The selectivity of probes can be evaluated by parallel comparison against a similar class of analytes. For example, Chang's group validated selectivity of their metal probes by carefully comparing various kinds of metal ions together with the target metal ions.[11] Many examples of diversity-oriented fluorescence sensors were discovered by in vitro fluorescence response assessments prior to their application in a biological system.[12,13] It is noteworthy that the fluorescence response profile against diverse analytes could provide ultimate selectivity information. While similar profiling approaches have been widely used in drug discovery,[14] their application to develop fluorescent sensors is still at an early stage.

The challenge of large-scale, quantitative investigation of fluorescence sensor development requires a practical high-throughput screening platform. For this, a microplate assay platform is chosen because of its unique advantages, such as simple adoption for any kind of analytes, flexible throughput control, and the homogeneous interaction between a sensor molecule and an analyte. To broaden the scope of fluorescent sensor discovery, we collected 10 classes of bioanalytes (total 94 individual analytes) for high-throughput in vitro screening and performed an assay in 384-well microplates. From the resulting profile, we identified fluorescent small molecule sensors for pH, human serum albumin (HSA), and total ribonucleic acid (RNA).

RESULTS AND DISCUSSION

Design of BDI Compounds. The endogenous GFP chromophore contains two aromatic moieties, a *para*-hydroxy benzene and an imidazolinone ring linked by a methine group. On the basis of these building block structures, 41 benzylideneimidazolinone (**BDI**) derivatives were synthesized with substitution patterns highlighted in Table 1. Since a lot of benzaldehyde building blocks are commercially available, we could easily maximize structural diversity of the R1 moiety. Each **BDI** compound shares a common core moiety; however, each analogue has distinct structures that may provide unique fluorescent turn-on phenomena by interacting with target molecules.

Synthesis of the **BDI**s was carried out by a 2 + 3 cycloaddition of the corresponding aromatic Schiff base with the imidate (Scheme 1c).[15]

Photophysical properties in solution. The spectroscopic properties of **BDI** compounds were examined and are summarized in Table 1. As previously reported, most **BDI** compounds show very low extinction coefficients and fluorescence quantum yields in ethanol. Each of these compounds absorbs in the visible range, with λ_{max} (abs) between 341 and 440 nm and has fluorescence emission ranging from 464 to 599 nm.

BDI compounds that consist of either 4-diethylamino (**BDI 24**) or 4-dimethylamino (**BDI 25, 33, 35**) exhibit significantly longer absorption max wavelengths than other derivatives ($\Delta\lambda_{abs}$ = 71.7 nm between the mean absorbance wavelength of **BDI 24**, **25**, **33**, and **35** compared to other compounds). The notable red shift of the absorbance indicates the elongated "push-pull" electronic conjugation from the aminobenzyl group.

High Throughput in Vitro Fluorescence Response Profiling toward Biorelevant Analytes. Prior to experimentation, the solubility of all compounds was validated in 100 μM concentration of HEPES buffer (20 mM HEPES with 1% of the DMSO stock solution at pH 7.4). Under these conditions, all 41 **BDI** compounds avoided precipitation, and the absorbance/fluorescence spectra exhibited reproducible peak shape in spite of their extremely weak extinction coefficients and low quantum yields.

To systematically investigate the fluorescence response profile of **BDI** compounds, 10 classes of analytes related to various biological processes were screened. The analyte classes were (i) pH standard solutions, (ii) viscous buffer solution, (iii) nucleotides and nucleosides, (iv) nucleic acids, (v) peptides, (vi) proteins, (vii) metal cations, (vii) oxidation−reduction related molecules, (viii) pesticides, and (ix) miscellaneous analytes, totaling 94 individual analyte molecules (Supporting Information, Table S2). Each analyte was tested at four serial concentrations together with a given concentration of **BDI** compounds to determine the dose response dependence on their endogenous concentration or

Scheme 1. Synthetic Scheme of BDI Compounds: (A) Synthesis of Aromatic Schiff Base, (B) Synthesis of Imidate, (C) Synthesis of BDIs[a]

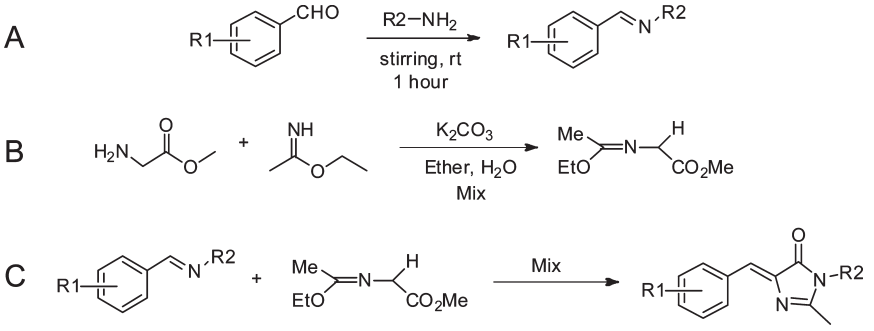

[a] Reactions were carried out by combining 1equiv of Schiff base and 1.1 equiv of the imidate under ambient conditions with magnetic stirring.[15]

Table 1. Substitution Patterns and Spectroscopic Properties of BDI Compounds[a]

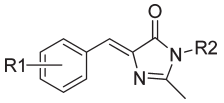

BDI #	R1	R2	λ_{abs} (nm)	λ_{em} (nm)	ε (M^{-1} cm^{-1})	ϕ
1	4-OH	Me	368	473	2,596	0.0060
2	4-OMe	Me	367	490	12,961	0.0018
3	4-OAc	Me	350	472	5,106	0.0045
4	4-CO_2H	Me	356	474	5,913	0.0085
5	4-OBz	Me	368	476	9,611	0.0020
6	3,5-*t*-Bu/4-OH	Me	373	471	8,888	0.0021
7	3-OH	Me	365	469	1,857	0.0247
8	2-(N)/4-OH	Me	359	481	3,805	0.0485
9	4-Me	Me	348	471	7,105	0.0044
10	3-Me	Me	348	468	5,499	0.0050
11	2-Me	Me	349	472	5,630	0.0034
12	2,4-Me	Me	352	472	5,630	0.0036
13	2,5-Me	Me	357	478	4,360	0.0041
14	4-Et	Me	353	478	6,733	0.0032
15	2-CF_3	Me	341	490	3,826	0.0455
16	3-OMe	Me	355	510	9,501	0.0041
17	2,3-OMe	Me	352	579	6,251	0.0471
18	2,4,5-OMe	Me	413	527	5,894	0.0111
19	2,5-OMe	Me	396	548	3,799	0.3062
20	4-NO_2	Me	376	599	4,869	0.2008
21	4-Cl	Me	352	472	6,598	0.0060
22	2-F	Me	351	475	6,299	0.0096
23	4-CN	Me	361	475	5,498	0.2490
24	4-$N(Et)_2$	Me	438	527	12,817	0.0065
25	4-$N(Me)_2$	Me	430	527	13,529	0.0029
26	1-naphthyl	Me	374	476	2,247	0.2080
27	2-naphthyl	Me	369	483	9,026	0.0048
28	2-quinoline	Me	372	476	3,784	0.0971
29	1-naphthyl	Et	378	464	5,214	0.0039
30	4-OH	*n*-Pr	369	476	10,783	0.0018
31	4-Me	*n*-Pr	351	470	8,334	0.0034
32	4-*i*-Pr	*n*-Pr	353	509	6,434	0.0039
33	4-$N(Me)_2$	*n*-Pr	433	504	8,604	0.0739
34	4-OH	*n*-Bu	371	476	10,739	0.0018
35	4-$N(Me)_2$	*n*-Bu	440	505	10,063	0.0650
36	4-OH	*n*-Pentyl	371	503	9,031	0.0019
37	4-OH	$C_3H_6N(Me)_2$	372	471	4,867	0.0029
38	4-OH	$C_3H_6N(Me)_3$	369	472	4,091	0.0035
39	4-OH	*n*-$C_{11}H_{22}OH$	369	554	8,007	0.0020
40	4-OH	*n*-C_{16}	371	504	6,723	0.0020
41	3-OH	*n*-C_{16}	353	474	3,328	0.0112

[a] All data were measured in ethanol with the presence of 1% DMSO as co-solvent. The fluorescence quantum yield was determined using FITC as a standard (Φ_{fl} = 0.93 in 0.1 M NaOH).

effective concentration, and these fluorescent emission intensities were compared with the value of chromophore itself in the buffer solution. Additionally, the entire concentration−response pattern was used for investigation of the selectivity among the different sets of analytes.

Fluorescence spectra were obtained using a monochromator-based fluorescence microplate reader not only to investigate emission spectra change, but also to increase throughput.[16] Excitation wavelengths of individual **BDI** molecules were determined based on their maximum wavelength of absorbance in

dx.doi.org/10.1021/co100012k |*ACS Comb. Sci.* 2011, 13, 32–38

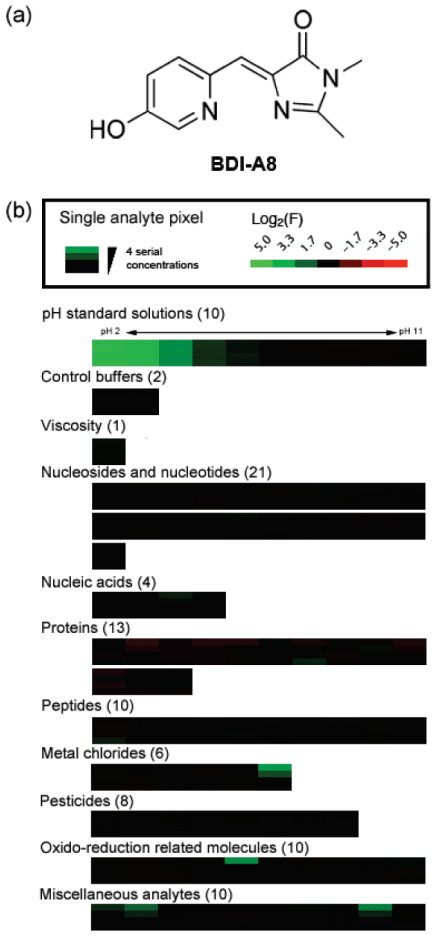

Figure 1. (a) Structure of **BDI 8**, and (b) in vitro fluorescence response profile of **BDI 8**. The number inside the parentheses indicates the number of individual analytes. Green color represents fluorescence intensity increase, and red color represents fluorescence decrease as denoted in the scale bar. Four serial concentrations were stacked in the same column in a dose dependent manner. Fluorescence intensity fold change was obtained at 520 nm (λ_{ex} = 370 nm). For a detail decoding table, refer to the Supporting Information, Table S3.

20 mM HEPES. It should be noted that maximum wavelength of excitation and emission used in vitro screening are different from the values in Table 1 because of the solvent effect. Fluorescence emission spectra were measured for all **BDI** compounds and 94 analytes at 4 concentrations. To facilitate the broad use of this data, a fluorescence response profile database was configured (Supporting Information, Figure S2). Primary screening results of total spectra were stored in the database, and changes to the emission spectrum were visualized by a heat map method. A heat map is a graphical representation of fluorescence fold change using two color codes to simplify complexity of data. Green represents an increase of emission intensity, while red represents a decrease in emission intensity. In this two-color profile, the fluorescence response pattern against 94 analytes could be easily evaluated. For instance, Figure 1b shows the in vitro fluorescence response profile of **BDI 8**, which showed strong pH dependence with a fluorescence increase in acidic media as well as showing a fluorescence increase in the presence of one metal cation and two miscellaneous analytes in a dose dependent manner. The concentration dependent response pattern is useful to evaluate the quality of an assay, and allows for the determination of

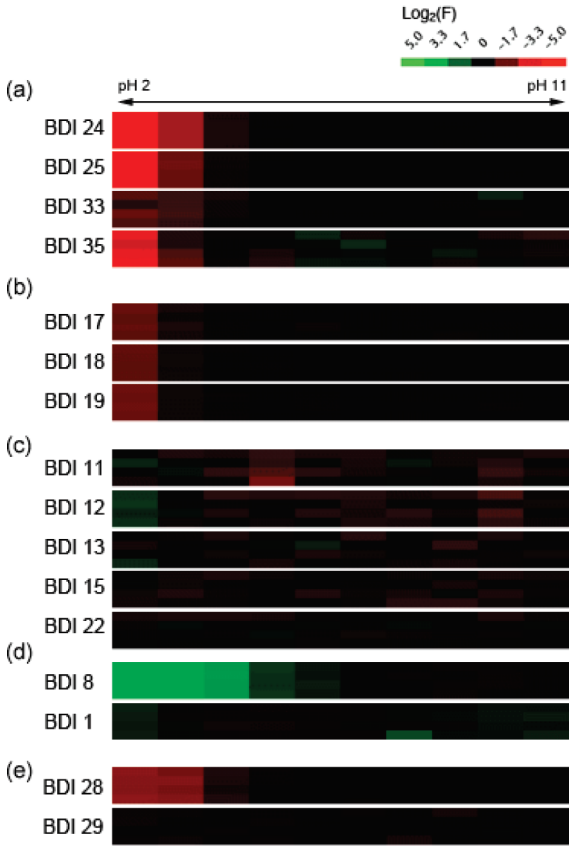

Figure 2. Heat map profiles of pH response from **BDI** compounds containing (a) *para*-amino benzyl, (b) *ortho*-methoxy moieties, and (c) other functional group in the *ortho* position. Fluorescence profile comparison between homocyclic and heterocyclic rings; (d) *p*-hydroxyl benzyl and *p*-hydroxyl pyridine derivatives, (e) naphthalene and quinoline derivatives.

dynamic ranges and sensitivity of probes.[17] For those analytes that showed remarked response, further experiments were pursued to determine the sensitivity for selective sensor application. The given profiles were analyzed for structure fluorescence response relationships.

Fluorescence Response Profile and Structural Relationship. The present profile allows for evaluation of the fluorescence intensity change of a given **BDI** compound with its structural building blocks. In pH profiles, all amino benzyl containing **BDI** compounds (**BDI 24** and **25**) revealed strong fluorescence quenching in acidic conditions, which most likely is induced by *N*-protonation (Figure 2a, $\Phi_{pH=2}^{BDI\ 24}$ = 0.002, $\Phi_{pH=7}^{BDI\ 24}$ = 0.021). Compounds containing different functional groups in the *ortho* position showed a distinct pH dependent pattern. Four functional moieties were compared within a given series of equivalent R2 substitutions including compounds of methyl (**BDI 11**, **12**, **13**), trifluoromethyl (**BDI 15**), fluoro- (**BDI 22**), and methoxy- (**BDI 17**, **18**, **19**), with fluorescence quenching in acidic solution observed for only *ortho*-methoxy compounds (Figure 2b,c). Single atom substitution in the aromatic ring also induced dramatic changes in the fluorescence response patterns. The wt-GFP chromophore, **BDI 1**, showed slight emission enhancement in basic media; however, its pyridine derivative, **BDI 8**, exhibited a strong emission enhancement in acidic solution (Figure 2d, $\Phi_{pH=2}^{BDI\ 8}$ = 0.786, $\Phi_{pH=7}^{BDI\ 8}$ =0.008). Likewise, we observed an emission decrease from the quinoline derivative (**BDI 28**), whereas the

dx.doi.org/10.1021/co100012k |*ACS Comb. Sci.* 2011, 13, 32–38

naphthalene derivative (**BDI 29**) showed minimal pH response (Figure 2e).

Similar structural analysis could also be performed based on the structure of analytes. Within the miscellaneous analyte class, primary amines caused fluorescence enhancement at high concentration for most **BDI** compounds (Supporting Information, Figure S3). Since the pH changes induced by two primary amines, dopamine and histamine, were already included in the pH profile, it is believed that **BDI** compounds share common interaction modes with those primary amines. Another notable response is the hydrophobic interaction with macromolecules. Many fluorescent small molecules, including 8-aminonaphthalenesulfonamide or rosamine compounds, show non-specific fluorescence increase to hydrophobic proteins such as albumin.[13] Conversely, most **BDI** compounds exhibited fluorescence quenching toward albumins. Considering the fluorescence enhancement in wt-GFP stimulated by rigidifying the chromophore structure, this profile implies that protein analytes do not have a common binding pocket for the **BDI** scaffold.

The results of these analyses demonstrate that the profiles generated are useful to analyze the relationship between fluorescence responses and structural characteristics in both analytes and probes. With this general response pattern information, we further sought to discover selective fluorescence turn-on sensors.

Fluorescence Sensor Discovery from the Profile. To be maximally useful, the fluorescence response profile should allow for the discovery of novel sensor molecules. Since we initially classified analytes in terms of the nature of the individual analyte, it was straightforward to compare fluorescence response within the same class of analytes. In this study, we found two sensor molecules from separate analyte classes that warranted further investigation.

(i). RNA Sensors. Although fluorescence small molecule sensors for nucleic acid macromolecules have been extensively used for cell imaging and sequencing, the continued development of improved sensors that can distinguish different kinds of nucleic acids is currently of great interest.[18] Accordingly, 4 kinds of nucleic acids were collected as a primary screening analyte class to discover sensors that could discriminate double strand DNA (dsDNA), single strand DNA (ssDNA), RNA, and *t*-RNA. First of all, we found **BDI 37** and **BDI 38** exhibited an increase in fluorescence emission for all four kinds of nucleic acids from the primary screening (Supporting Information, Figure S4). **BDI 38** contain a positively charged linker in the **BDI** derivatives, and it has strong Coulomb interaction with all negatively charged nucleic acids.

Primary hit compounds that enhanced emission in the presence of RNA compared to DNA were further tested to confirm primary profiles, and 3 **BDI** compounds revealed selectivity toward total RNA. Interestingly, all selected RNA sensors, **BDI 2**, **BDI 3**, and **BDI 5**, contain alkyloxy/aryloxy groups (-OR) at the *para* position in the R1 moiety. These findings suggest that the *para*-alkyloxy group plays a role in distinguishing RNAs over DNAs in **BDI** scaffolds. We also note that the *para*-alkoxy groups played a significant role in enhancing the fluorescence in the solid state.[18] Among the three primary hits, the *para*-methoxy group brought not only the highest fold change in fluorescence to total RNA, but also exceptionally low cross reactivity to other nucleic acids (Figure 3). When we tested these hit compounds toward different 16-mer RNA oligomers, they generally exhibited higher fluorescence increment toward "AU" rich oligomers (Supporting Information, Figure S6). Although we observed a response trend

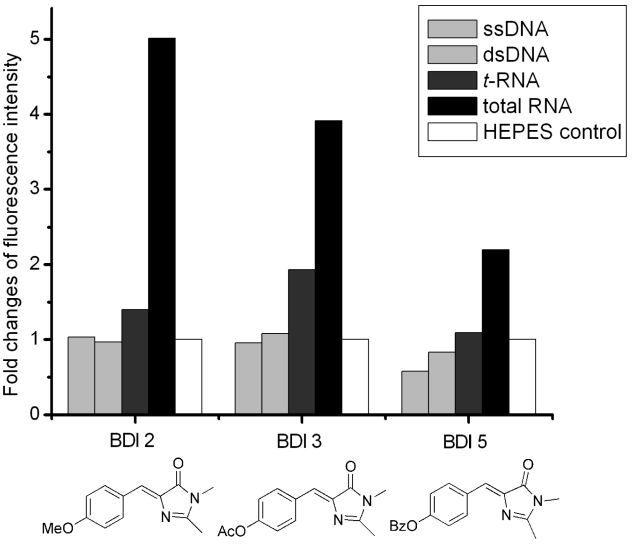

Figure 3. Fluorescence intensity fold changes of (a) **BDI 2** at λ_{em} 512 nm, (b) **BDI 3**, and (c) **BDI 5** at λ_{em} 532 nm against 4 nucleic acids at 1 mg/mL final concentrations in 20 mM HEPES (pH 7.4). Full emission spectra (Supporting Information, Figure S5).

against "AU" rich oligomers, it is still not clear which specific RNA sequences were necessary for selective recognition of each compound or how these compounds were interacting with total RNA mixture in solution. However, this example clearly shows that large-scale profiling could identify novel modes of interaction between sensor molecule and analyte. Such studies are currently in progress.

(ii). Human Serum Albumin (HSA) Sensors. As mentioned earlier, most **BDI** compounds showed fluorescence quenching toward many proteins (Supporting Information, Figure S7). Noticeable primary hit compounds were **BDI 24** and **BDI 25**. These two compounds, which contain a dialkylamino motif, showed clear emission enhancement to human serum albumin (HSA) in a dose dependent manner.

HSA is the most abundant protein in human blood plasma (60% of total plasma protein) and is known to bind to diverse exogenous drug molecules by hydrophobic interactions.[19] Since **BDI 24** exhibited a greater fold increase, we further examined the bindings between HSA and **BDI 24**. In the presence of HSA, the maximum wavelength of fluorescence emission was blue-shifted from 530 to 515 nm, while the intensity increased by 10.4 fold (Figure 4a, Supporting Information, Figure S8). This hypsochromic shift can be caused by solvatochromism, the reduction of non-radiative decay, or the perturbation of electronic conjugation system through the binding with HSA. To further investigate the binding properties of HSA and **BDI 24** quantitatively, various concentrations of **BDI 24** were titrated with HSA, and a fractional saturation curve revealed a dissociation constant (K_d) of 3.57 μM (Figure 4b).

CONCLUSION

Although the sensitivities displayed here do not compare to others for the same proteins, they are based upon a limited initial set of chromophores. Nevertheless, this study represents the first example of small molecule fluorescence sensor discovery utilizing the green fluorescent protein chromophores by large-scale fluorescence profiling. We believe this profiling approach could accelerate the fluorescence sensor discovery process for other

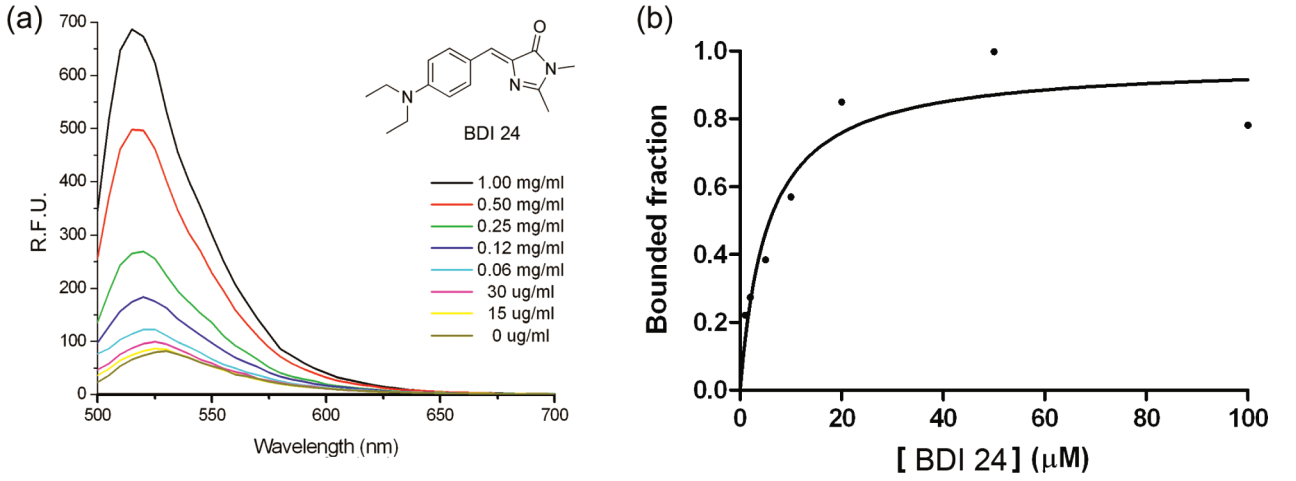

Figure 4. Fluorescence titration analysis for the binding of **BDI 24** with HSA. (a) Fluorescence spectral change of **BDI 24** (100 uM) upon addition of the HSA in 20 mM HEPES buffer (pH 7.4). (b) Fractional saturation curve of **BDI 24** with HSA. The dissociation constant was measured using 7.5 μM HSA. Experimental K_d = 3.57 μM.

fluorescent scaffolds, since the diversity of the fluorophores introduced here represents a very small fraction of the potential structural space. In the current report, we have demonstrated the use of the fluorescence response pattern based sensor discovery utilizing the green fluorescent protein chromophore and its derivatives. Forty-one structurally related **BDI** compounds were synthesized and exploited for the generation of fluorescence response profiles toward 10 classes of analytes or a total of 94 individual biologically relevant analytes. From the large-scale fluorescence profile, the structural moieties that induce specific pH response were identified as well as those showing a unique response pattern to specific analytes. Further experiments exhibited a selective fluorescence emission enhancement upon interaction between **BDI 24** with HSA (K_d = 3.57 μM) and **BDI 2** with total RNA, which showed a marked selectivity with a 5-fold emission increase. The use of more carefully focused recognition elements should increase the sensitivity and approach the on/off ratio of GFP itself. For instance, we now have increased the sensitivity to the hydrophobic "octa acid" by another factor of 10.[20] Further studies are currently in progress.

EXPERIMENTAL SECTION

Materials and Methods. All the materials were obtained from commercial suppliers (Aldrich) and used without further purification. The solvents used for the spectroscopy experiments were of spectrophotometric grade. Spectroscopic properties of compounds and in vitro high-throughput screenings were performed on SpectraMax M2 plate reader (Molecular Devices Inc.).

Quantum Yield Measurements. Quantum yields were calculated by measuring the integrated emission area of the fluorescent spectra and comparing that value to the area measured for FITC in EtOH when excited at 489 nm (Φ_{FITC} = 0.93). Quantum yields for the BDI compounds were then calculated using eq 1, where F represents the area of fluorescent emission, n is reflective index of the solvent, and Abs is absorbance at excitation wavelength selected for standards and samples.

$$\Phi_{flu}^{sample} = \Phi_{fl}^{reference}\left(\frac{F^{sample}}{F^{reference}}\right)\left(\frac{\eta^{sample}}{\eta^{reference}}\right)\left(\frac{\mathrm{Abs}^{reference}}{\mathrm{Abs}^{sample}}\right) \quad (1)$$

In Vitro Fluorescence Screening. **BDI** compounds (100 μM) were screened in 20 mM HEPES, pH 7.4. Fluorescence intensities were measured using a SpectraMax M2 plate reader in 384-well format. Excitation was provided at each compound's excitation range, and emission was obtained starting from at least 30 nm longer wavelengths from the excitation. All the analytes were tested at four serial concentrations depending on the endogenous concentration of the analyte (Supporting Information, Table S2). Every analyte was prepared the same day prior to the fluorescence experiment to minimize sample contamination. For detailed protocols refer to the Supporting Information.

Determination of the Dissociation Constant. The fluorescent emission spectra with various concentrations of **BDI** compounds were measured on a SpectraMax M2 plate reader. The fluorescent titration curve was fitted to the standard equation using Graphpad Prism v5 software. The bound fraction (X) of fluorescent sensor at each concentration was determined using the eq 2

$$X = \frac{F_c - F_o}{F_{sat} - F_o} \quad (2)$$

where F_c and F_o are the fluorescence intensities of a given concentration of **BDI** compounds with and without target analyte, respectively. F_{sat} is the fluorescence intensity at the same concentration of **BDI** compounds when fully bound with target analyte. F_{sat} was determined by fluorescence titration at each concentration with a series concentration of analyte. The results were plotted according to a non-linear fitting curve eq 3

$$F = F_o + (F_{sat} - F_o)([\mathrm{BDI}])/(K_D + [\mathrm{BDI}]) \quad (3)$$

where K_D is dissociation constant, and [BDI] is the concentration of the **BDI** compound.

ASSOCIATED CONTENT

Supporting Information. Detail characterizations of all **BDI** compounds, in vitro screening procedures/results, and complete refs 14a, 14d. This material is available free of charge via the Internet at http://pubs.acs.org.

dx.doi.org/10.1021/co100012k |ACS Comb. Sci. 2011, 13, 32–38

AUTHOR INFORMATION

Corresponding Author

*E-mail: chmcyt@nus.edu.sg.

Author Contributions

▽These authors contributed equally to this work.

ACKNOWLEDGMENT

This work was supported by an intramural funding from A*STAR Biomedical Research Council and National University of Singapore (Young Investigator Award: R-143-000-353-123). J.-S.L. thanks the POSCO TJ Park Foundation (TJ Park Bessemer Science Fellowship) for the generous support. L.M.T. thanks the National Science Foundation through Grants CHE-0809179 for financial support. A.B. acknowledges the Center for Organic Photonics and Electronics (COPE) at Georgia Tech for a graduate research fellowship.

REFERENCES

(1) Tsien, R. Y. *Annu. Rev. Biochem.* **1998,** *67*, 509–544.

(2) Heim, R.; Prasher, D. C.; Tsien, R. Y. *Proc. Natl. Acad. Sci. U.S.A.* **1994,** *91*, 12501–12504.

(3) (a) Mandal, D.; Tahara, T.; Meech, S. R. *J. Phys. Chem. B* **2004,** *108*, 1102–1108. (b) Kummer, A. D.; Kompa, C.; Niwa, H.; Hirano, T.; Kojima, S.; Michel-Beyerle, M. E. *J. Phys. Chem. B* **2002,** *106*, 7554–7559. (c) Webber, N. M.; Litvinenko, K. L.; Meech, S. R. *J. Phys. Chem. B* **2001,** *105*, 8036–8039.

(4) (a) Stoner-Ma, D.; Jaye, A. A.; Matousek, P.; Towrie, M.; Meech, S. R.; Tonge, P. J. *J. Am. Chem. Soc.* **2005,** *127*, 2864–2865. (b) Agmon, N. *Biophys. J.* **2005,** *88*, 2452–2461.

(5) Stoner-Ma, D.; Melief, E. H.; Nappa, J.; Ronayne, K. L.; Tonge, P. J.; Meech, S. R. *J. Phys. Chem. B* **2006,** *110*, 22009–22018.

(6) (a) Hu, C. D.; Chinenov, Y.; Kerppola, T. K. *Mol. Cell* **2002,** *9*, 789–798. (b) Hynes, T. R.; Tang, L.; Mervine, S. M.; Sabo, J. L.; Yost, E. A.; Devreotes, P. N.; Berlot, C. H. *J. Biol. Chem.* **2004,** *279*, 30279–30286. (c) Shaffer, J. M.; Hellwig, S.; Smithgall, T. E. *Biochemistry* **2009,** *48*, 4780–4788.

(7) Domaille, D. W.; Que, E. L.; Chang, C. J. *Nat. Chem. Biol.* **2008,** *4*, 507–507.

(8) Wu, L. X.; Burgess, K. *J. Am. Chem. Soc.* **2008,** *130*, 4089–4096.

(9) Chen, K. Y.; Cheng, Y. M.; Lai, C. H.; Hsu, C. C.; Ho, M. L.; Lee, G. H.; Chou, P. T. *J. Am. Chem. Soc.* **2007,** *129*, 4534–4535.

(10) Baldridge, A.; Samanta, S. R.; Jayaraj, N.; Ramamurthy, V.; Tolbert, L. M. *J. Am. Chem. Soc.* **2010,** *132*, 1498–1499.

(11) (a) Yoon, S.; Miller, E. W.; He, Q.; Do, P. H.; Chang, C. J. *Angew. Chem., Int. Ed.* **2007,** *46*, 6658–6661. (b) He, Q.; Miller, E. W.; Wong, A. P.; Chang, C. J. *J. Am. Chem. Soc.* **2006,** *128*, 9316–9317. (c) Zeng, L.; Miller, E. W.; Pralle, A.; Isacoff, E. Y.; Chang, C. J. *J. Am. Chem. Soc.* **2006,** *128*, 10–11. (d) Yoon, S.; Albers, A. E.; Wong, A. P.; Chang, C. J. *J. Am. Chem. Soc.* **2005,** *127*, 16030–16031.

(12) (a) Lee, J. S.; Kim, Y. K.; Vendrell, M.; Chang, Y. T. *Mol. BioSyst.* **2009,** *5*, 411–421. (b) Wang, S.; Kim, Y. K.; Chang, Y. T. *J. Comb. Chem.* **2008,** *10*, 460–465. (c) Ahn, Y. H.; Lee, J. S.; Chang, Y. T. *J. Am. Chem. Soc.* **2007,** *129*, 4510–4511. (d) Li, Q.; Lee, J. S.; Ha, C.; Park, C. B.; Yang, G.; Gan, W. B.; Chang, Y. T. *Angew. Chem., Int. Ed.* **2004,** *43*, 6331–6335.

(13) Ahn, Y. H.; Lee, J. S.; Chang, Y. T. *J. Comb. Chem.* **2008,** *10*, 376–380.

(14) (a) Lamb, J.; et al. *Science* **2006,** *313*, 1929–1935. (b) Paull, K. D.; Shoemaker, R. H.; Hodes, L.; Monks, A.; Scudiero, D. A.; Rubinstein, L.; Plowman, J.; Boyd, M. R. *J. Natl. Cancer Inst.* **1989,** *81*, 1088–1092. (c) Weinstein, J. N.; Kohn, K. W.; Grever, M. R.; Viswanadhan, V. N.; Rubinstein, L. V.; Monks, A. P.; Scudiero, D. A.; Welch, L.; Koutsoukos, A. D.; Chiausa, A. J. *Science* **1992,** *258*, 447–451. (d) Hughes, T. R.; et al. *Cell* **2000,** *102*, 109–126.

(15) (a) Dong, J.; Solntsev, K. M.; Poizat, O.; Tolbert, L. M. *J. Am. Chem. Soc.* **2007,** *129*, 10084–10085. (b) Kojima, S.; Ohkawa, H.; Hirano, T.; Maki, S.; Niwa, H.; Ohashi, M.; Inouye, S.; Tsuji, F. I. *Tetrahedron Lett.* **1998,** *39*, 5239–5242.

(16) Simeonov, A.; Jadhav, A.; Thomas, C. J.; Wang, Y.; Huang, R.; Southall, N. T.; Shinn, P.; Smith, J.; Austin, C. P.; Auld, D. S.; Inglese, J. *J. Med. Chem.* **2008,** *51*, 2363–2371.

(17) Inglese, J.; Shamu, C. E.; Guy, R. K. *Nat. Chem. Biol.* **2007,** *3*, 438–441.

(18) (a) O'Connor, N. A.; Stevens, N.; Samaroo, D.; Solomon, M. R.; Marti, A. A.; Dyer, J.; Vishwasrao, H.; Akins, D. L.; Kandel, E. R.; Turro, N. J. *Chem. Commun.* **2009,** 2640–2642. (b) Li, Q.; Kim, Y.; Namm, J.; Kulkarni, A.; Rosania, G. R.; Ahn, Y. H.; Chang, Y. T. *Chem. Biol.* **2006,** *13*, 615–623. (c) Lee, J. W.; Jung, M.; Rosania, G. R.; Chang, Y. T. *Chem. Commun.* **2003,** 1852–1853.

(19) (a) Kragh-Hansen, U.; Chuang, V. T.; Otagiri, M. *Biol. Pharm. Bull.* **2002,** *25*, 695–704. (b) Min, J.; Lee, J. W.; Ahn, Y. H.; Chang, Y. T. *J. Comb. Chem.* **2007,** *9*, 1079–1083.

(20) Baldridge, A.; Samanta, A.; Jayaraj, N.; Ramamurthy, V.; Tolbert, L. M., submitted.